neuroglia

MDPI

Article

Brain-Homing Peptide Expression on the Membrane Enhances the Delivery of Exosomes to Neural Cells and Tissue

Jonhoi Smith [1], Melvin Field [2] and Kiminobu Sugaya [1,*]

[1] Burnett School of Biomedical Sciences, College of Medicine, University of Central Florida, Orlando, FL 32816, USA; jonhoi.smith@ucf.edu
[2] Neurosurgery, AdventHealth, Orlando, FL 32804, USA
* Correspondence: ksugaya@ucf.edu

Abstract: Background/Objectives: Glioblastoma (GBM), a highly aggressive grade IV astrocytoma, poses a major therapeutic challenge due to the resistance of cancer stem cells (CSCs) existing within its cell population to the conventional therapies. Recently, we reported that RNA interference targeting CSC protection mechanism significantly improved therapeutic efficacy. However, challenges remain, including limited transfection efficiency in neural cells and the difficulty of crossing the blood–brain barrier (BBB). Methods: In this study, we investigated the potential of exosome-mediated delivery of therapeutic cargo to GBM cells by engineering the exosomes to carry green fluorescent protein (GFP) and expressing brain-homing peptide (BHP) on their surface, which has high affinity to the neural cells. Results: We found that BHP-modified exosomes doubled GFP delivery efficacy from 20% to 40%, outperforming traditional transfection methods like lipofection in vitro. In vivo, BHP-modified exosomes demonstrated an ability to cross the BBB and targeted cargo delivery to brain regions following intranasal and subcutaneous administration. Conclusions: These results underscore the potential of engineered exosomes for efficient cargo delivery to enhance therapeutic efficacy against brain tumors and suggest novel avenues for delivering biomolecules to the brain in the treatment of neurological disorders.

Keywords: exosomes; brain-homing peptide; glioblastoma; drug delivery system

Academic Editor: Sadayuki Hashioka

Received: 6 November 2024
Revised: 18 December 2024
Accepted: 30 December 2024
Published: 4 January 2025

Citation: Smith, J.; Field, M.; Sugaya, K. Brain-Homing Peptide Expression on the Membrane Enhances the Delivery of Exosomes to Neural Cells and Tissue. *Neuroglia* **2025**, *6*, 3. https://doi.org/10.3390/neuroglia6010003

1. Introduction

Glioblastoma (GBM) is the most common and aggressive type of brain tumor with newly diagnosed patients having a median survival of only about 15 months despite receiving standard treatment [1]. The poor prognosis of GBM is largely due to its heterogenetic nature, which is characterized by a wide range of genetic and molecular characteristics that drive resistance to therapy [2]. Cancer stem cells (CSCs), a distinct subset of tumor cells with stem cell-like properties, play a major role in driving therapeutic resistance and facilitating tumor recurrence. As a result, targeting and eliminating CSCs has become a central focus in developing more effective treatments, aimed at overcoming resistance and lowering the risk of relapse.

A key challenge in developing effective CSC treatments is identifying viable therapeutic targets, particularly those involved in drug resistance [3,4], and aberrant signaling pathways in CSCs [5–8]. We reported that factors maintaining stemness are highly expressed in GBM CSCs compared to normal neural stem cells (NSCs) or GBM cells [9]. Reducing these stemness factors with RNAi significantly enhanced the efficacy of chemotherapy in treating GSCs [10]. RNAi holds great potential for treatment because of its gene-specific targeting ability and wide range of application [11]. However, delivering RNAi molecules

to the brain is challenging. Delivering drugs to the brain has long been challenging due to the blood–brain barrier (BBB), a selectively permeable membrane that protects the central nervous system and blocks over 90% of small drug molecules [12]. This barrier significantly limits treatment options for brain conditions. A promising solution to overcome this challenge is to use extracellular vesicles (EVs) as delivery vehicles.

EVs are lipid-bound vesicles secreted by cells and consist of several subtypes, including exosomes, microvesicles, and apoptotic bodies [13]. Each subtype shares similar characteristics but differs in biogenesis, size, and cargo [13,14]. Exosomes, the smallest subtype of extracellular vesicles, ranging from 30 to 150 nm in size, are secreted by various cell types and are now recognized as vital for intercellular communication, carrying a diverse array of macromolecules as cargo [15], which can alter the biological profile of target cells [16–18]. Naturally produced by cells, exosomes can diffuse across cell membranes to deliver their cargo, reducing immune response and cellular toxicity [19]. Furthermore, exosomes can be extracted from various bodily fluids, including urine, saliva, breast milk, and plasma [20–23], highlighting their potential for diagnostic applications [24,25]. We previously found that CSC-secreted exosomes contain NANOG family retro-oncogene NANOGP8 with a distinct upstream gene sequence [26,27]. While much research is currently focused on exosomes for diagnostic purposes; their unique physiology also makes them highly valuable for targeted drug delivery [28]. To improve the exosome's ability to target cells of the central nervous system is by adding a brain-homing peptide, which is a short amino acid sequence that is reported to increase the affinity of a nanoparticle to neural tissue [29].

In this study, we demonstrate that the exosomes can effectively deliver their cargo, GFP, to patient-derived primary GBM cells in vitro and cross the BBB, reaching the brain from peripheral injection in vivo. Our results suggest that exosomes can serve as effective vehicles for targeted drug delivery to neural cells within the brain via peripheral administration.

2. Materials and Methods

2.1. Cell Culture

Primary glioblastoma cells were obtained from tumor tissue excised during surgery from a patient with GBM, following approved protocols from the AdventHealth Hospital and the University of Central Florida Institutional Review Boards. Informed consent was obtained from participants, and strict adherence to Health Insurance Portability and Accountability Act (HIPAA) regulations was maintained. Cells were cultured as spheroids in human neural stem cell (HNSC) media, consisting of Dulbecco's modified eagle medium/nutrient mixture F-12 (DMEM/F12) (Gibco™, Waltham, MA, USA) with heparin (0.5 U/mL) (Sagent Pharmaceuticals, Schaumburg, IL, USA), epidermal growth factor (EGF) (20 ng/mL) (R&D Systems, Minneapolis, MN, USA), basic fibroblast growth factor (bFGF) (20 ng/mL) (R&D Systems, Minneapolis, MN, USA), and 2% B27 (Gibco™, Waltham, MA, USA). All cultures were maintained at 37 °C with 5% CO_2. Once spheroids reached approximately 1 mm in diameter, they were dissociated using Accutase (Gibco™, Waltham, MA, USA). Subsequently, $CD133^+$ cells were isolated using $CD133^+$ antibody-conjugated magnetic microbeads (Miltenyi Biotec, Bergisch Gladbach, Germany), following the manufacturer's protocol. The $CD133^+$ cells were then cultured in HNSC media for further proliferation.

HEK 293 (ATCC, Manassas, VA, USA) and HEK 293TN (System Biosciences, Palo Alto, CA, USA) cells were cultured in Dulbecco's modified eagle medium (DMEM) (Corning, NY, USA) supplemented with 10% fetal bovine serum (FBS) (Corning, NY, USA), 2 mM L-glutamine, and 1× nonessential amino acids with 1% (*v*/*v*) antibiotics, penicillin–streptomycin (Gibco™, Waltham, MA, USA), were added. The cells were seeded into

culture flasks at a density of approximately 5×10^4 cells/cm^2 and then incubated at 37 °C with 5% CO_2. The medium was replaced every 2–3 days.

2.2. Production of Lentivirus

To produce lentiviral particles, HEK 293TN cells were seeded in culture dishes or flasks to reach 75–90% confluency by transfection time. The transfer plasmid containing the gene of interest, such as the XPack GFP (System Biosciences, Palo Alto, CA, USA) or XStamp BHP (System Biosciences, Palo Alto, CA, USA), was co-transfected with packaging plasmids (pLP1) and an envelope plasmid (VSV-G) into HEK 293TN cells using Lipofectamine™ 2000 (ThermoFisher, Waltham, MA, USA) according to the manufacturer's instructions. The transfer plasmid containing XPack GFP encodes a fusion protein that shuttles GFP into exosomes. The XStamp was used to express BHP to the surface of the exosomes. Plasmids were combined with the transfection reagent in serum-free media and added to the cells, which were incubated at 37 °C with 5% CO_2. Transfection efficiency was assessed 24 h later by observing fluorescent-positive cells if a fluorescent marker was included. Starting 24 h post-transfection, culture media containing viral particles were collected every 24 h for three days, with fresh media added after each collection. The collected viral supernatant was stored at 4 °C until all collections were complete. To concentrate the virus, PEG-it™ Virus Precipitation Solution (System Biosciences, Palo Alto, CA, USA) was added to the pooled viral supernatant, followed by incubation at 4 °C for overnight, and then centrifugation (1500× *g* for 30 min at 4 °C) to pellet the viral particles. The viral pellet was resuspended in PBS, aliquoted to prevent repeated freeze–thaw cycles, and stored at −80 °C for long-term use.

2.3. Lentiviral Transduction

HEK 293 cells were seeded in culture dishes or flasks to reach 75–90% confluency, achieving an optimal density for lentiviral particle production. Lentiviral particles containing the XPack GFP and/or XStamp BHP constructs were then added to the cultures at an appropriate multiplicity of infection and incubated overnight (12–16 h) at 37 °C with 5% CO_2 to ensure effective viral entry and integration. The following day, the culture medium was replaced with fresh growth media to remove residual virus and minimize cellular stress. Successful transduction was verified by GFP expression observed under a fluorescence microscope 24–48 h after infection. For the selection of cells expressing the gene of interest, 1 µg/mL puromycin was added to the culture medium. Cells were subsequently maintained in puromycin-containing media, with media changes every 2–3 days, to eliminate non-transduced cells and enrich for cells expressing the gene of interest.

2.4. Exosome Isolation from the Media

Exosomes were isolated from conditioned culture media using a modified PEG-NaCl precipitation method. Briefly, 20 mL of conditioned culture media was first centrifuged at 3000× *g* for 30 min at 4 °C to remove cell debris. The supernatant was then combined with 20 mL of 20% PEG containing 375 mM NaCl and incubated overnight at 4 °C to promote exosome precipitation. The following day, the mixture was centrifuged at 10,000× *g* for 60 min at 4 °C, yielding an exosome pellet. Exosome concentration was determined by measuring protein absorbance at 280 nm (A280) using a NanoDrop spectrophotometer (ThermoFisher, Waltham, MA, USA).

2.5. Western Blot

Proteins were extracted from cells and exosomes using RIPA buffer (Invitrogen, Waltham, MA, USA) containing a protease and phosphatase inhibitor. Protein concentration was assessed using the Pierce™ BCA Protein Assay Kit (ThermoFisher, Waltham, MA, USA)

according to the manufacturer's protocol. Total protein was separated by electrophoresis on NuPAGE 4–12% Bis-Tris gels (Invitrogen, Waltham, MA, USA) and wet-transferred onto a PVDF membrane. The membrane was blocked with a blocking solution Tris-Buffered Saline 2% Tween 20 (TBST) with 4% low-fat milk for 1 h at room temperature with agitation. Before blocking, the PVDF membrane was activated by pre-wetting in 100% methanol for 1 min, followed by soaking in ddH_2O for 2 min and then in TBST for 5 min. TurboGFP (Origene, Rockville, MD, USA, Cat: TA150071) and β-Actin (Cell Signaling, Danvers, MA, USA, Cat: 4970L) primary antibodies were diluted in the blocking solution at 1:2000 and 1:4000 concentration, respectively, and incubated overnight at 4 °C with agitation. The secondary antibody (Goat anti-Rabbit HRP, Cat: 31460) was also diluted in the blocking solution at 1:20,000 concentration and incubated for 1 h at room temperature. Images were acquired using the ChemiDoc MP Imaging System (BioRad, Hercules, CA, USA).

2.6. Dot Blot Analysis to Detect GFP in the Brain Tissue

Exosomes containing GFP and expressing BHP (400 μg) on their surface were intranasally administered to NOD *scid* gamma immunodeficient mice (NSG) (The Jackson Laboratory, Bar Harbor, ME, USA). After 4 h of the administration, the mice were perfused with saline, and their brains were dissected for protein extraction. Protein samples were prepared by dissolving the tissue using RIPA buffer (Invitrogen, Waltham, MA, USA) containing protease and phosphatase inhibitors. Protein concentration was assessed using the Pierce™ BCA Protein Assay Kit (ThermoFisher, Waltham, MA, USA) following manufacturer's protocol. The lysed sample was spotted within a nitrocellulose membrane. The membrane was left to dry for 1 h at RT and blocked with a blocking solution, 4% low-fat milk in TBST for 1 h at RT with agitation. The primary antibody TurboGFP (Origene, Rockville, MD, USA, Cat: TA150071) was diluted in a blocking solution at 1:2000 concentration and then incubated overnight at 4 °C. The secondary antibody (goat anti-rabbit HRP) was diluted at 1:25,000 concentration in the blocking solution and incubated for 1 h at RT. Images were captured using the ChemiDoc MP Imaging System (BioRad, Hercules, CA, USA).

2.7. Flow Cytometry

$CD133^+$ GBM cells were seeded at 500,000 cells per well in 6-well plates. Exosomes containing GFP and/or BHP were added (100 μg protein per well) and incubated overnight. The following day, cells were dissociated into a single-cell suspension using Accutase, washed with PBS, and analyzed in the FITC channel (450/45 nm) using the CytoFlex flow cytometer (Beckman Coulter, Brea, CA, USA). The experiment was performed in triplicate.

2.8. Detection of GFP in the Brain Using Fluorescent Microscopy

Exosomes containing GFP and expressing BHP (400 μg) on their surface were subcutaneously administered to C57BL/6 mice (The Jackson Laboratory, Bar Harbor, ME, USA). After 4 h of administration, the mice were perfused with saline, and their brains were dissected for protein extraction. Subsequently, these brains were harvested and sliced into 40 μm slices, and GFP fluorescent signals in the brain were examined using a Keyence BZ-X800 microscope (Keyence, Itasca, IL, USA).

2.9. Single-Particle Interferometric Reflectance Imaging Sensing

The size distribution and surface markers of exosomes were analyzed using a Leprechaun® instrument (Unchained Laboratories, Pleasanton, CA, USA), following the manufacturer's guidelines. Briefly, the Leprechaun's Luni consumable captures exosomes from a sample by using antibodies that bind specifically to CD9, CD63, or CD81 surface proteins. Following this capture, the Luni Washer was used to remove any unbound par-

ticles. Fluorescent antibodies for CD9, CD63, or CD81 were then applied to counterstain the exosomes. The Leprechaun's software 1.1was used to analyze the exosomes, assessing their sizes, concentrations, and phenotypes.

3. Results

3.1. Expression of XPack GFP Gene Enables Packaging of GFP into Exosomes Derived from HEK 293 Cells

We produced exosomes that endogenously packed GFP by transducing HEK 293 cells with lentiviral particles containing the XPack GFP gene. To select cells stably expressing the desired gene, cells were treated with G418. Fluorescent microscopy confirmed the generation of a homogenous population of GFP-expressing cells (Figure 1B). Typically, the transfection of a gene containing a fluorescent marker results in diffuse fluorescence throughout the cell. However, the XPack gene is engineered to shuttle the target protein specifically into exosomes, resulting in GFP localization within the cytosol, which suggests GFP is being incorporated into vesicles. Exosomes were collected from conditioned media of the producer cell line, cultured with exosome-depleted FBS, and isolated for further analysis. Lysates from both HEK 293 cells and HEK 293 cells expressing XPack GFP were used for Western blot analysis, which confirmed the presence of GFP in the EVs from the XPack GFP-expressing cells (Figure 1C).

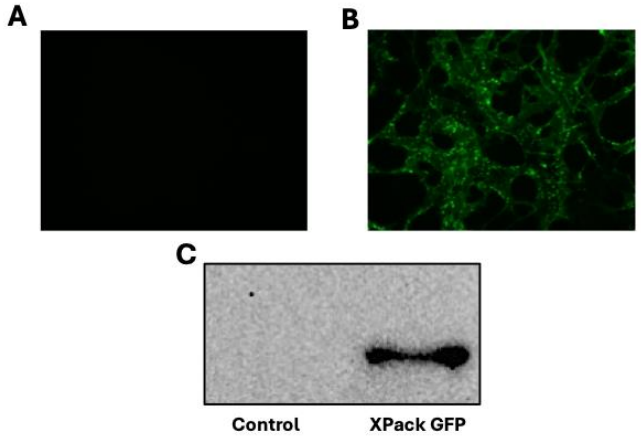

Figure 1. Fluorescent microscopy images of HEK 293 cells showing (**A**) non-transfected cells and (**B**) cells transfected with XPack GFP. (**C**) Western blot analysis showing GFP detection in HEK 293 exosome lysate, isolated using the PEG precipitation method.

3.2. PEG Precipitation Causes Aggregation of Exosomes Derived from Culture Media

To ensure successful cargo delivery, we analyzed exosomes from conditioned culture media (non-processed) and exosomes isolated using the PEG method (processed). Exosome samples were captured using the exosomal tetraspanin marker CD81 and analyzed with the Leprechaun system. In Figure 2A, we present a representative image showing an abundance of vesicles evenly distributed in the non-processed sample when captured with CD81, with no signal in the isotype control. An image of PEG-processed exosomes captured with the CD81 antibody also shows a high abundance of exosomes, while the isotype control displays no signal. Although both samples contain a substantial number of particles, a significant level of aggregation is observed in the PEG-isolated exosomes. For exosome delivery, we aimed to measure the concentration increase after PEG isolation. Exosome concentrations were determined by capturing antibodies for exosomal tetraspanin markers CD9, CD63, and CD81. In the non-processed sample, particle concentrations were 6.32×10^8, 6.09×10^8, and 8.99×10^8 particles/mL when captured with CD9, CD63, and

CD81, respectively (Figure 2B). Once processed, EV concentrations increased to 1.8×10^9, 2.68×10^9, and 2.38×10^9 particles/mL, respectively (Figure 2B).

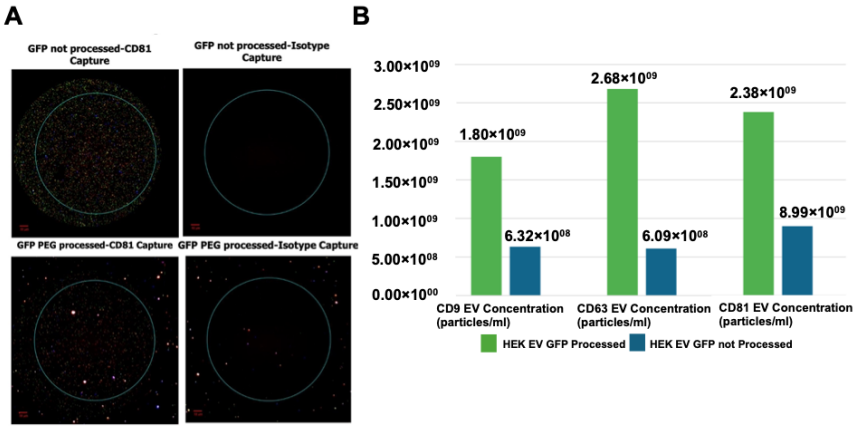

Figure 2. (**A**) A representative image of extracellular vesicles captured with the CD81 antibody from non-processed conditioned media and PEG-processed conditioned media. (**B**) A bar graph and a chart showing exosome concentration (particles/mL) for exosomes captured using CD9, CD63, and CD81 antibodies, with the blue bars representing non-processed conditioned media and the green bars representing PEG-processed conditioned media. A chart detailing the concentration of exosome samples captured with CD9, CD63, and CD81 antibodies.

3.3. Size Profile Analysis Reveal That Most Exosomes Are Smaller than 80 nm

Exosomes are typically 30–150 nm in size [13]. To determine whether PEG processing altered the size of our particles, EVs were captured using the tetraspanin markers CD9, CD63, and CD81, and the size profile of individual particles was assessed. We have analyzed the dispersity using dynamic light scattering (DLS). After PEG processing, we confirmed that the exosomes maintained a monodisperse distribution. Consistent with previous findings, PEG processing increased the concentration of particles per mL. Our results indicate that the majority of particles in both processed and non-processed samples were between 30 and 100 nm in size (Figure 3).

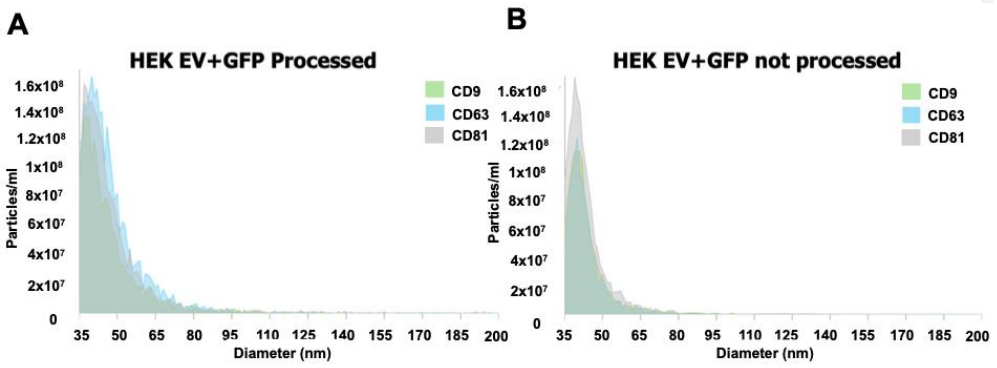

C

Sample name	CD9 EV mean size (nm)	CD9 EV mode size (nm)	CD63 EV mean size (nm)	CD63 EV mode size (nm)	CD81 EV mean size (nm)	CD81 EV mode size (nm)
HEK EV GFP processed	47.8	38	48.4	40	47.8	37
HEK GFP not processed	44.6	40	43.8	40	44.1	39

Figure 3. The size profile analysis of exosomes captured based on CD9, CD63, and CD81 markers is shown as follows: (**A**) HEK293 (XPack GFP) exosomes processed using the PEG method, (**B**) HEK293 (XPack GFP) exosomes not processed using the PEG method, and (**C**) table displaying the mean and mode sizes of exosomes captured by CD9, CD63, and CD81 markers.

3.4. BHP Enhance GFP Delivery to Patient-Derived Glioma Stem Cells In Vitro

Cells of the neural lineage are known to be difficult to transfect. Therefore, we wanted to measure the efficiency of exosome transfection to GSCs. We found that GBM cells positive for the CD133 marker also express several embryonic stem cell genes [9,10]. Therefore, cells positive for the CD133 marker were considered as CSCs in our study. Using the XPack GFP vector, we successfully packed GFP into exosomes and delivered the cargo to GSCs. To quantify the percentage of cells successfully transfected with GFP after exosome treatment, we employed flow cytometry, analyzing only single cells within the population as determined by forward and side scatter. A minimum of 10,000 events were recorded, and the percentage of GFP-positive cells was calculated based on the count of fluorescent-positive cells within the single-cell population. Approximately 20% of the GSC population exhibited a GFP signal following treatment with XPack GFP exosomes (Figure 4A). Given the typically low transfection rates in stem cells, we sought to improve cargo delivery efficacy through exosomes. To achieve this, we modified the exosome surface by adding a brain-homing peptide (BHP). HEK 293 cells were co-transduced with XStamp BHP, which incorporates a brain-homing peptide on the exosome surface, and XPack GFP. With the addition of BHP, GFP uptake in GSCs increased, doubling the proportion of GFP-positive cells from 20% to 40% ($p = 0.000158$), thereby demonstrating a significant enhancement in cargo delivery efficiency.

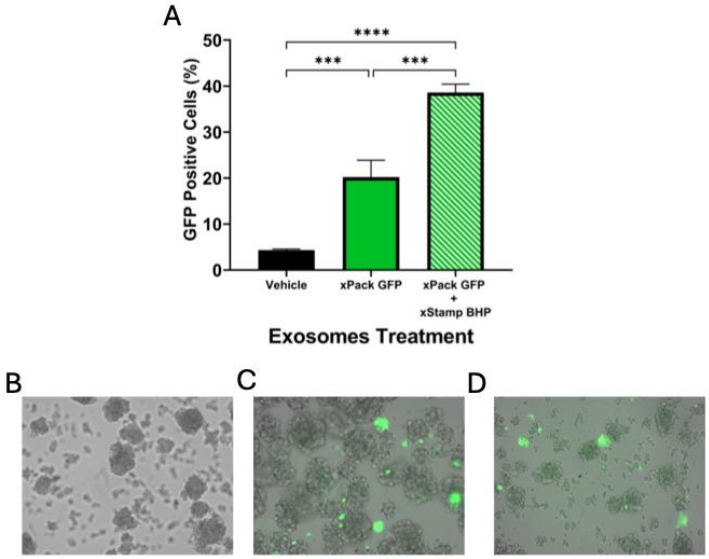

Figure 4. (**A**) Flow cytometry analysis showing the percentage of GFP-positive cells following treatment with HEK 293 exosomes, HEK 293 exosomes (XPack GFP), and HEK 293 exosomes (XPack GFP + XStamp BHP). Fluorescent microscopy images of GBM CSCs post-exosome treatment: (**B**) control, (**C**) XPack GFP, and (**D**) XPack GFP + XStamp BHP. Dot blot analysis for GFP detection from brain lysates of NSG mice treated with HEK 293 (XStamp BHP) and HEK 293 (XPack GFP + XStamp BHP) exosomes. Statistical analysis was performed using a one-way ANOVA followed by Holm–Sidaks multiple comparison test. Significance levels were indicated as *** $p < 0.001$ and **** $p < 0.0005$.

3.5. BHP Enables HEK293-Derived Exosomes to Bypass Blood–Brain Barrier In Vivo, Facilitating GFP Delivery to Brain

To assess whether these exosomes could cross the BBB and deliver cargo to brain cells, we treated FAD and NSG mice with exosomes carrying GFP. Brain tissue lysates from animals treated with BHP and BHP/GFP exosomes were analyzed by dot blot. As shown in Figure 5A, GFP was detected in the BHP/GFP sample following intranasal exosome administration to NSG mice. Additionally, we administered the exosomes subcutaneously, behind the head of the mice, to determine whether GFP could be detected in the brain.

Following subcutaneous injection, fluorescent microscopy confirmed GFP presence in the brains of FAD mice, specifically showing signal localization within the hippocampal region.

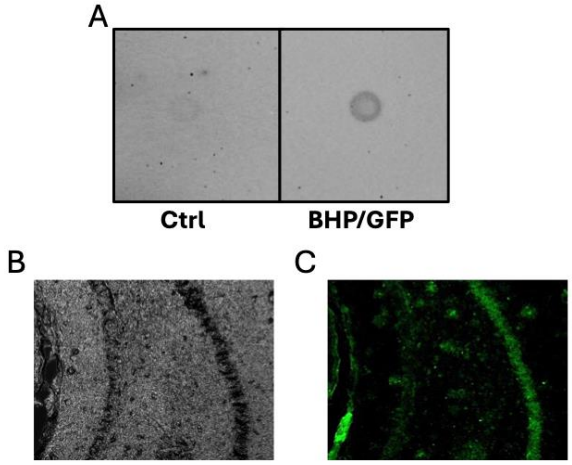

Figure 5. (**A**) The dot blot analysis of brain tissue lysates from NSG mice treated intranasally with exosomes derived from HEK293 cells expressing XStamp BHP and co-expressing XStamp BHP/XPack GFP. (**B**) The microscopy image of the hippocampal region of FAD mice treated subcutaneously with exosomes from HEK293 cells co-expressing XStamp BHP/XPack GFP. (**C**) The fluorescent microscopy image of the hippocampal region in FAD mice treated subcutaneously with exosomes from HEK293 cells co-expressing XStamp BHP/XPack GFP.

4. Discussion

Inhibiting genes with RNA interference (RNAi) shows great potential in the field of molecular therapeutics. Using shRNA, we improved the efficacy of chemotherapeutic treatment against GSCs in vitro [10]. In this study, lentivirus was the vector that delivered the silencing RNA. However, viruses are limited due to their lack of ability to cross the BBB and can elicit a strong immune response [30]. Thus, there is a need for a vehicle to carry these gene-silencing molecules.

The use of exosomes as drug delivery vehicles represents a significant paradigm shift from traditional liposomal systems. While liposomes are the most extensively researched lipid-based drug carriers, their use is associated with notable drawbacks, including high production cost, short half-life, and drug leakage [31]. Moreover, their efficacy in clinical applications, such as cancer treatment, is limited due to a lack of selectivity [32]. In contrast liposomes, which are synthetically produced, exosomes are derived from cells, granting them intrinsic targeting capabilities and natural biocompatibility that synthetic systems lack. Although targeted liposomes were once considered as a revolutionary approach two decades ago, their limited success highlights the challenges synthetic delivery systems face in achieving effective therapeutic outcomes.

Exosomes demonstrate a clear advantage in this regard. For instance, Kamerkar et al. showed that CD47-expressing exosomes facilitated more effective delivery to pancreatic tumor cells in vivo compared to liposomes [33]. Exosomes also possess the unique ability to cross biological barriers, such as the BBB, making them particularly promising for clinical applications in treating neurological disorders. Furthermore, clinical trials data reveal no significant adverse effects in the treatment of Alzheimer's disease, cancer, and stroke [34–36].

Recent advancement in exosome engineering have further expanded their potential. For example, Alvarez-Erviti et al. demonstrated tissue-specific targeting through peptides displayed on exosomal membranes [37]. Our approach builds upon these advancements, offering a novel strategy that combines exosome engineering with precision targeting. The

development of exosome technology is still an emerging field with immense promise. Various methods are being developed to load exosomes with specific therapeutic cargo [38,39], while rigorous quality controls ensure the absence of residual viral vectors in accordance with GMP standards, resulting in particles that are safe for therapeutic administration [40].

Exosomes sourced appropriately exhibit low cytotoxicity and minimal immune response [41–43]. However, production challenges remain a critical factor in their therapeutic application. The current isolation methods often yield low quantities and compromised purity. Recent advancements, including large-scale production methods, such as bioreactors and microfluidic platforms, aim to address these limitations and enable the production of high-quality nanovesicles at scale [44–46]. As these technologies mature, exosomes are poised to revolutionize drug delivery, offering a safer and more efficient alternative to traditional systems.

This study demonstrates the potential of exosome-mediated delivery as a highly effective platform for targeted therapies, especially in treating central nervous system (CNS) disorders. By expressing the XPack GFP gene in HEK 293 cells, we successfully incorporated GFP into exosomes, enabling fluorescent tracking of these vesicles. The integration of GFP into exosomes was confirmed through fluorescent microscopy, which revealed GFP localization in the cytosol, likely within vesicles, rather than diffusely throughout the cells. Western blot analysis further validated GFP's presence in exosome lysates, confirming the successful packaging of GFP within the exosomes. This selective targeting and packaging highlight the versatility of the XPack system in directing desired molecules into exosomes.

The exosome isolation process, specifically using PEG precipitation, was also assessed. Although PEG precipitation effectively increased exosome concentration, it led to notable aggregation. This aggregation may impact exosome functionality and delivery efficacy, suggesting that while PEG isolation enhances concentration, it requires further optimization to maintain exosome integrity. Non-processed exosomes showed evenly distributed particles captured by CD81, while PEG-processed samples showed a higher particle concentration but with some aggregation. For future applications, balancing concentration increase and particle integrity will be essential for therapeutic delivery.

Size profiling indicated that the majority of the exosomes remained within the expected 30–100 nm range, even after PEG processing. This size stability aligns with typical exosome characteristics, reinforcing that PEG processing does not alter the overall particle size profile, a critical consideration for their functionality as delivery vectors.

The application of BHP on exosome surfaces represents a significant advancement for CNS-targeted delivery. Exosomes modified with XStamp BHP exhibited enhanced delivery of GFP to patient-derived CSCs, nearly doubling the GFP-positive cell population from 20% to 40%. This substantial increase underscores the potential of BHP-modified exosomes to improve cargo delivery efficiency, even to challenging targets like GSCs. Future studies should explore additional peptide modifications or combinatory approaches to further optimize exosome-based delivery for therapeutic applications.

In vivo results further confirm the potential of BHP-modified exosomes to cross the BBB and deliver therapeutic cargo to the brain. GFP was detected in the brain tissue of both FAD and NSG mice following intranasal and subcutaneous administration, with GFP signals localized in the hippocampal region in FAD mice. This ability to bypass the BBB and deliver cargo to specific brain regions is promising for the development of CNS therapies, particularly for neurodegenerative diseases. The BHP modification not only enhances the targeting capacity of exosomes but also facilitates non-invasive delivery methods, which could be particularly valuable in clinical settings.

Overall, our findings underscore the potential of exosome-based delivery systems, particularly when combined with targeting peptides like BHP, to overcome the limitations of

conventional drug delivery to the CNS. The exosomes developed in this study offer distinct advantages over those described in the literature. These include enhanced neural tissue targeting facilitated by brain-homing peptide expression, effective crossing of the BBB, and maintained size and structural stability following PEG processing. These attributes position them as highly promising candidates for targeted drug delivery to the brain. However, optimizing isolation methods, enhancing targeting efficiency, and validating therapeutic outcomes in further in vivo studies remain essential next steps. This study provides a foundational approach for developing exosome-mediated therapies for CNS diseases, potentially improving treatment outcomes in future clinical applications.

5. Conclusions

Developing effective therapies for central nervous system disorders presents a unique challenge due to BBB, which restricts many molecules from passing through. This is where exosomes, the body's natural couriers, show remarkable potential. These nano vesicles can cross cellular boundaries, making them ideal vehicles for targeted drug delivery to the brain. In this study, we explore the transformative potential of exosomes as carriers for brain-targeted therapies. Future research will focus on refining delivery conditions and pioneering biomolecule delivery, paving the way for innovative treatments that could significantly enhance patients' quality of life.

Author Contributions: Conceptualization, K.S.; methodology, K.S., M.F. and J.S.; validation, K.S., M.F. and J.S.; formal analysis, J.S.; investigation, J.S.; resources, K.S. and M.F.; data curation, J.S.; writing—original draft preparation, J.S.; writing—review and editing, K.S.; visualization, J.S.; supervision, K.S.; project administration, K.S.; funding acquisition, K.S. All authors have read and agreed to the published version of the manuscript.

Funding: This research was funded by Florida Cancer Innovation Fund by The Florida Department of Health (Grant number: MOABC) for Kiminobu Sugaya.

Institutional Review Board Statement: The study was conducted in accordance with the guidelines of The Privacy Rule issued under a law called the Health Insurance Portability and Accountability Act of 1996 (HIPAA) and approved by the Institutional Review Board of the University of Central Florida and Neuro-oncology center, AdventHealth (formerly known as Florida Hospital) IRB #2319-0832.

Informed Consent Statement: Before enrollment in the study, informed consent was obtained from the participating patients. The informed consent was compliant with applicable federal regulations (including FDA 21 CFR 50.20-50.27 and DHHS 45 CFR 46) and approved by AdventHealth and the University of Central Florida Institutional Review Boards (IRB).

Data Availability Statement: The data presented in this study are available in the article. The original law data are available on request from the corresponding author.

Conflicts of Interest: The authors declare no conflicts of interest.

References

1. Rončević, A.; Koruga, N.; Soldo Koruga, A.; Rončević, R.; Rotim, T.; Šimundić, T.; Kretić, D.; Perić, M.; Turk, T.; Štimac, D. Personalized Treatment of Glioblastoma: Current State and Future Perspective. *Biomedicines* **2023**, *11*, 1579. [CrossRef] [PubMed]
2. Kim, H.; Zheng, S.; Amini, S.S.; Virk, S.M.; Mikkelsen, T.; Brat, D.J.; Grimsby, J.; Sougnez, C.; Muller, F.; Hu, J.; et al. Whole-genome and multisector exome sequencing of primary and post-treatment glioblastoma reveals patterns of tumor evolution. *Genome Res.* **2015**, *25*, 316–327. [CrossRef]
3. Wang, N.; Wang, Z.; Peng, C.; You, J.; Shen, J.; Han, S.; Chen, J. Dietary compound isoliquiritigenin targets GRP78 to chemosensitize breast cancer stem cells via β-catenin/ABCG2 signaling. *Carcinogenesis* **2014**, *35*, 2544–2554. [CrossRef]
4. Venere, M.; Hamerlik, P.; Wu, Q.; Rasmussen, R.D.; Song, L.A.; Vasanji, A.; Tenley, N.; Flavahan, W.A.; Hjelmeland, A.B.; Bartek, J.; et al. Therapeutic targeting of constitutive PARP activation compromises stem cell phenotype and survival of glioblastoma-initiating cells. *Cell Death Differ.* **2014**, *21*, 258–269. [CrossRef]

5. Zhao, Z.; Lu, P.; Zhang, H.; Xu, H.; Gao, N.; Li, M.; Liu, C. Nestin positively regulates the Wnt/β-catenin pathway and the proliferation, survival and invasiveness of breast cancer stem cells. *Breast Cancer Res.* **2014**, *16*, 408. [CrossRef] [PubMed]
6. Venkatesh, V.; Nataraj, R.; Thangaraj, G.S.; Karthikeyan, M.; Gnanasekaran, A.; Kaginelli, S.B.; Kuppanna, G.; Kallappa, C.G.; Basalingappa, K.M. Targeting Notch signalling pathway of cancer stem cells. *Stem Cell Investig.* **2018**, *5*, 5. [CrossRef] [PubMed]
7. Burnett, J.P.; Lim, G.; Li, Y.; Shah, R.B.; Lim, R.; Paholak, H.J.; McDermott, S.P.; Sun, L.; Tsume, Y.; Bai, S.; et al. Sulforaphane enhances the anticancer activity of taxanes against triple negative breast cancer by killing cancer stem cells. *Cancer Lett.* **2017**, *394*, 52–64. [CrossRef] [PubMed]
8. Yu, D.; Shin, H.S.; Lee, Y.S.; Lee, Y.C. miR-106b modulates cancer stem cell characteristics through TGF-β/Smad signaling in CD44-positive gastric cancer cells. *Lab. Invest.* **2014**, *94*, 1370–1381. [CrossRef]
9. Field, M.; Alvarez, A.; Bushnev, S.; Sugaya, K. Embryonic stem cell markers distinguishing cancer stem cells from normal human neuronal stem cell populations in malignant glioma patients. *Clin. Neurosurg.* **2010**, *57*, 151–159.
10. Smith, J.; Field, M.; Sugaya, K. Suppression of NANOG Expression Reduces Drug Resistance of Cancer Stem Cells in Glioblastoma. *Genes* **2023**, *14*, 1276. [CrossRef]
11. Traber, G.M.; Yu, A.M. RNAi-Based Therapeutics and Novel RNA Bioengineering Technologies. *J. Pharmacol. Exp. Ther.* **2023**, *384*, 133–154. [CrossRef]
12. Pardridge, W.M. The blood-brain barrier: Bottleneck in brain drug development. *NeuroRx* **2005**, *2*, 3–14. [CrossRef]
13. Doyle, L.M.; Wang, M.Z. Overview of Extracellular Vesicles, Their Origin, Composition, Purpose, and Methods for Exosome Isolation and Analysis. *Cells* **2019**, *8*, 727. [CrossRef]
14. Hadizadeh, N.; Bagheri, D.; Shamsara, M.; Hamblin, M.R.; Farmany, A.; Xu, M.; Liang, Z.; Razi, F.; Hashemi, E. Extracellular vesicles biogenesis, isolation, manipulation and genetic engineering for potential in vitro and in vivo therapeutics: An overview. *Front. Bioeng. Biotechnol.* **2022**, *10*, 1019821. [CrossRef]
15. Kalluri, R.; LeBleu, V.S. The biology, function, and biomedical applications of exosomes. *Science* **2020**, *367*, eaau6977. [CrossRef] [PubMed]
16. Vaidya, M.; Sreerama, S.; Gonzalez-Vega, M.; Smith, J.; Field, M.; Sugaya, K. Coculture with Neural Stem Cells May Shift the Transcription Profile of Glioblastoma Multiforme towards Cancer-Specific Stemness. *Int. J. Mol. Sci.* **2023**, *24*, 3242. [CrossRef] [PubMed]
17. Sayeed, N.; Sugaya, K. Exosome mediated Tom40 delivery protects against hydrogen peroxide-induced oxidative stress by regulating mitochondrial function. *PLoS ONE* **2022**, *17*, e0272511. [CrossRef] [PubMed]
18. Valerio, L.S.A.; Sugaya, K. Xeno- and transgene-free reprogramming of mesenchymal stem cells toward the cells expressing neural markers using exosome treatments. *PLoS ONE* **2020**, *15*, e0240469. [CrossRef] [PubMed]
19. Chen, R.; Xu, X.; Qian, Z.; Zhang, C.; Niu, Y.; Wang, Z.; Sun, J.; Zhang, X.; Yu, Y. The biological functions and clinical applications of exosomes in lung cancer. *Cell Mol. Life Sci.* **2019**, *76*, 4613–4633. [CrossRef]
20. Wang, Y.; Zhang, M. Urinary Exosomes: A Promising Biomarker for Disease Diagnosis. *Lab. Med.* **2023**, *54*, 115–125. [CrossRef]
21. Li, K.; Lin, Y.; Luo, Y.; Xiong, X.; Wang, L.; Durante, K.; Li, J.; Zhou, F.; Guo, Y.; Chen, S.; et al. A signature of saliva-derived exosomal small RNAs as predicting biomarker for esophageal carcinoma: A multicenter prospective study. *Mol. Cancer* **2022**, *21*, 21. [CrossRef] [PubMed]
22. Mirza, A.H.; Kaur, S.; Nielsen, L.B.; Størling, J.; Yarani, R.; Roursgaard, M.; Mathiesen, E.R.; Damm, P.; Svare, J.; Mortensen, H.B.; et al. Breast Milk-Derived Extracellular Vesicles Enriched in Exosomes from Mothers with Type 1 Diabetes Contain Aberrant Levels of microRNAs. *Front. Immunol.* **2019**, *10*, 2543. [CrossRef]
23. Li, Y.; Lyu, P.; Ze, Y.; Li, P.; Zeng, X.; Shi, Y.; Qiu, B.; Gong, P.; Yao, Y. Exosomes derived from plasma: Promising immunomodulatory agents for promoting angiogenesis to treat radiation-induced vascular dysfunction. *PeerJ* **2021**, *9*, e11147. [CrossRef]
24. Manterola, L.; Guruceaga, E.; Gállego Pérez-Larraya, J.; González-Huarriz, M.; Jauregui, P.; Tejada, S.; Diez-Valle, R.; Segura, V.; Samprón, N.; Barrena, C.; et al. A small noncoding RNA signature found in exosomes of GBM patient serum as a diagnostic tool. *Neuro Oncol.* **2014**, *16*, 520–527. [CrossRef]
25. Ji, Q.; Ji, Y.; Peng, J.; Zhou, X.; Chen, X.; Zhao, H.; Xu, T.; Chen, L.; Xu, Y. Increased Brain-Specific MiR-9 and MiR-124 in the Serum Exosomes of Acute Ischemic Stroke Patients. *PLoS ONE* **2016**, *11*, e0163645. [CrossRef] [PubMed]
26. Vaidya, M.; Kimura, A.; Bajaj, A.; Sugaya, K. 3′-UTR Sequence of Exosomal NANOGP8 DNA as an Extracellular Vesicle-Localization Signal. *Int. J. Mol. Sci.* **2024**, *25*, 7294. [CrossRef] [PubMed]
27. Vaidya, M.; Bacchus, M.; Sugaya, K. Differential sequences of exosomal NANOG DNA as a potential diagnostic cancer marker. *PLoS ONE* **2018**, *13*, e0197782. [CrossRef]
28. Song, Y.; Kim, Y.; Ha, S.; Sheller-Miller, S.; Yoo, J.; Choi, C.; Park, C.H. The emerging role of exosomes as novel therapeutics: Biology, technologies, clinical applications, and the next. *Am. J. Reprod. Immunol.* **2021**, *85*, e13329. [CrossRef]
29. Pasqualini, R.; Ruoslahti, E. Organ targeting in vivo using phage display peptide libraries. *Nature* **1996**, *380*, 364–366. [CrossRef]
30. Ali Zaidi, S.S.; Fatima, F.; Ali Zaidi, S.A.; Zhou, D.; Deng, W.; Liu, S. Engineering siRNA therapeutics: Challenges and strategies. *J. Nanobiotechnol.* **2023**, *21*, 381. [CrossRef]

31. Daraee, H.; Etemadi, A.; Kouhi, M.; Alimirzalu, S.; Akbarzadeh, A. Application of liposomes in medicine and drug delivery. *Artif. Cells Nanomed. Biotechnol.* **2016**, *44*, 381–391. [CrossRef]
32. Kim, E.M.; Jeong, H.J. Liposomes: Biomedical Applications. *Chonnam Med. J.* **2021**, *57*, 27–35. [CrossRef] [PubMed]
33. Kamerkar, S.; LeBleu, V.S.; Sugimoto, H.; Yang, S.; Ruivo, C.F.; Melo, S.A.; Lee, J.J.; Kalluri, R. Exosomes facilitate therapeutic targeting of oncogenic KRAS in pancreatic cancer. *Nature* **2017**, *546*, 498–503. [CrossRef]
34. Surana, R.; LeBleu, V.S.; Lee, J.J.; Smaglo, B.G.; Zhao, D.; Lee, M.S.; Wolff, R.A.; Overman, M.J.; Mendt, M.C.; McAndrews, K.M.; et al. Phase I study of mesenchymal stem cell (MSC)-derived exosomes with $KRAS^{G12D}$ siRNA in patients with metastatic pancreatic cancer harboring a $KRAS^{G12D}$ mutation. *J. Clin. Oncol.* **2022**, *40*, TPS633. [CrossRef]
35. Xie, X.; Song, Q.; Dai, C.; Cui, S.; Tang, R.; Li, S.; Chang, J.; Li, P.; Wang, J.; Li, J.; et al. Clinical safety and efficacy of allogenic human adipose mesenchymal stromal cells-derived exosomes in patients with mild to moderate Alzheimer's disease: A phase I/II clinical trial. *Gen. Psychiatr.* **2023**, *36*, e101143. [CrossRef] [PubMed]
36. Dehghani, L.; Khojasteh, A.; Soleimani, M.; Oraee-Yazdani, S.; Keshel, S.H.; Saadatnia, M.; Saboori, M.; Zali, A.; Hashemi, S.M.; Soleimani, R. Safety of Intraparenchymal Injection of Allogenic Placenta Mesenchymal Stem Cells Derived Exosome in Patients Undergoing Decompressive Craniectomy Following Malignant Middle Cerebral Artery Infarct, A Pilot Randomized Clinical Trial. *Int. J. Prev. Med.* **2022**, *13*, 7. [CrossRef] [PubMed]
37. Alvarez-Erviti, L.; Seow, Y.; Yin, H.; Betts, C.; Lakhal, S.; Wood, M.J. Delivery of siRNA to the mouse brain by systemic injection of targeted exosomes. *Nat. Biotechnol.* **2011**, *29*, 341–345. [CrossRef]
38. Sharma, V.; Mukhopadhyay, C.D. Exosome as drug delivery system: Current advancements. *Extracell. Vesicle* **2024**, *3*, 100032. [CrossRef]
39. Zeng, H.; Guo, S.; Ren, X.; Wu, Z.; Liu, S.; Yao, X. Current Strategies for Exosome Cargo Loading and Targeting Delivery. *Cells* **2023**, *12*, 1416. [CrossRef] [PubMed]
40. Wang, P.; Arntz, O.J.; Husch, J.F.A.; Kraan, P.M.V.; Beucken, J.; van de Loo, F.A.J. Polyethylene glycol precipitation is an efficient method to obtain extracellular vesicle-depleted fetal bovine serum. *PLoS ONE* **2023**, *18*, e0295076. [CrossRef]
41. Xia, Y.; Zhang, J.; Liu, G.; Wolfram, J. Immunogenicity of Extracellular Vesicles. *Adv. Mater.* **2024**, *36*, e2403199. [CrossRef]
42. Sun, L.; Xu, R.; Sun, X.; Duan, Y.; Han, Y.; Zhao, Y.; Qian, H.; Zhu, W.; Xu, W. Safety evaluation of exosomes derived from human umbilical cord mesenchymal stromal cell. *Cytotherapy* **2016**, *18*, 413–422. [CrossRef] [PubMed]
43. Fu, W.; Lei, C.; Liu, S.; Cui, Y.; Wang, C.; Qian, K.; Li, T.; Shen, Y.; Fan, X.; Lin, F.; et al. CAR exosomes derived from effector CAR-T cells have potent antitumour effects and low toxicity. *Nat. Commun.* **2019**, *10*, 4355. [CrossRef]
44. Kink, J.A.; Bellio, M.A.; Forsberg, M.H.; Lobo, A.; Thickens, A.S.; Lewis, B.M.; Ong, I.M.; Khan, A.; Capitini, C.M.; Hematti, P. Large-scale bioreactor production of extracellular vesicles from mesenchymal stromal cells for treatment of acute radiation syndrome. *Stem Cell Res. Ther.* **2024**, *15*, 72. [CrossRef] [PubMed]
45. Bai, J.; Wei, X.; Zhang, X.; Wu, C.; Wang, Z.; Chen, M.; Wang, J. Microfluidic strategies for the isolation and profiling of exosomes. *TrAC Trends Anal. Chem.* **2023**, *158*, 116834. [CrossRef]
46. Gao, J.; Li, A.; Hu, J.; Feng, L.; Liu, L.; Shen, Z. Recent developments in isolating methods for exosomes. *Front. Bioeng. Biotechnol.* **2022**, *10*, 1100892. [CrossRef] [PubMed]